MATEC Web of Conferences **36**, 02003 (2015)
DOI: 10.1051/matecconf/20153602003

Study of the Bloodstains in the Shroud of Turin: Chromatic Analysis and Possible Interpretation

Gabriele Bedon[1,a], Matteo Linguanotto[1], Ivan Simionato[1], and Francesco Zara[1]

[1] *University of Padua, Department of Industrial Engineering, Via Venezia 1, 35131 Padova, Italy*

Abstract. This work presents a chromatic characterization of the bloodstains of the Shroud of Turin. The analysis is carried out by considering the chromatic values of the bloodstains and by calculating the chromatic ratios to be adopted in a comparative analysis. Six categories were obtained and characterized. By considering the geometry of the body and the position of the sheet, the analysis allowed the formulation of hypotheses on the dynamics of blood formation and flowing.

1 Introduction

The Shroud of Turin (ST) is a linen cloth which shows the image of a man who appears to be buried after being crucifixed. This man is believed to be Jesus of Nazareth. The wish to understand the origins, the history and the authenticity of this relic involves any branch of science. The problem of dating [1–4], the formation of the image [5–7] and the identity [8, 9] of the Man of the Shroud (MS) are the issues which mostly emerge during this research which involves Science and Religion [10–12]. Since the co-presence of these two large cultural areas, a separation of the religious aspects from the scientific ones is necessary: this analysis is purely scientific. This study analyzes, from a chromatic point of view, the stains which are largely distributed on the whole sheet by processing high definition pictures.

The tests carried out on 1973 did not reveal the presence of blood on the stains visible on the ST, as reported by McCrone [13]. Following tests independently performed by Adler [14] and by Baima Bollone [15] since 1978 with more modern techniques gave, instead, a positive result, and showed that the blood is of human type: in particular, presence of hemoglobin and other blood specific substances were found [16].

The bloodstains are already the subject of high-pitched discussions, not only concerning their peculiarities, but also their formation and etiology. This research focuses on the chromatic aspects, which was made possible thanks to high definition images of the ST taken in 2002 by G. Durante. The aim of this work is the compilation of a ”map” reproducing the chromatic compatibility areas: this map is useful to formulate hypotheses concerning the formation of the stains.

[a] e-mail: gabriele.bedon@dii.unipd.it

Article available at http://www.matec-conferences.org or http://dx.doi.org/10.1051/matecconf/20153602003

2 Methodology

The stain analysis was based on a high definition digital photographs taken in 2002 by G. Durante, and processed with the software GIMP [17]. The software provided values of Red, Green and Blue pixels (RGB) for each chromatic level (8 bit image, 256 colors levels) of the selected zone, represented in a histogram. The average level for each color and the standard deviation were also calculated. The average values were made dimensionless by calculating the level ratios q_{RG} of Red/Green (R/G) and q_{RB} of Red/Blue (R/B).

Through the Kline-McClintock (KMC) formula [18], with the hypothesis of disconnected values:

$$i_q = \pm \sqrt{\sum (\Theta_i \cdot i_{xi})^2} \tag{1}$$

where the sensibility rate Θ_i has been considered as:

$$\Theta_i = \frac{\delta q}{\delta x_i} \tag{2}$$

the standard deviation i_{xi} of the average values x_i was propagated to obtain the standard deviation i_q of the ratios q.

The ratios were represented in plots to point out the compatibility zones. For each of them, an average with the relative uncertainty was then calculated: the KMC values were divided by the square root of the number of the data and multiplied by a K extension factor of 2.

Different sampling methods were adopted, depending on the stain characteristics with respect to size, position and clearness. Two different categories were found by a preliminary analysis of the sheet, probably linked to different fluid properties. On one hand, stains covering only warps were found, which are named ”localized” stains. On the other hand, stains with a greater size and covering both warps and weft were found, which are named ”diffused” stains.

- **”Localized” bloodstains**

  Many areas of the ST are characterized by segments more colored than background, see Figure 1. In order to capture only the chromatic ratios linked to the fluid, source of these stains, the RGB values were sampled by considering these segments. These stains were located in correspondence of arms, feet, face and side, both in the front and in the back image.

- **”Diffused” bloodstains**

  Some areas of the ST are characterized by spots where the color is not visible as segments, but it overlaps also the background color. In this case, the color analysis was based on a limited area of the stains, as shown in Figure 2. Diffused stains are located in correspondence of the back and the glutes.

R/B ratios were plotted against R/G ratios and groups were highlighted. These plots show the compatibility between different points. The average of the nearest points was afterwards calculated and the ratio values for every group was compared.

Figure 1. Pixel sampling for ”localized” stains.

Figure 2. Pixel sampling for ”diffused” stains.

3 Results

Following the procedure explained in Section 2, 60 compatibility groups were detected in various parts of the ST. A different color was assigned to each group, whose location in the original images can be found in Figures 3 and 4 [19]. Figure 5 shows the plot of the ratios. The different ratios areas are highlighted as follows:

- solid colors: average ratios are representative of the whole area and are supposed to be blood;
- dashed colors with labels: average ratios are representative of the whole area and are supposed not to be blood (G1, G2, G3, G4).
- dashed white: average ratios are not representative of the whole area and therefore were not included in Figure 5.

Each solid color is associated to the maximum and minimum ratios of its group in Table 1.

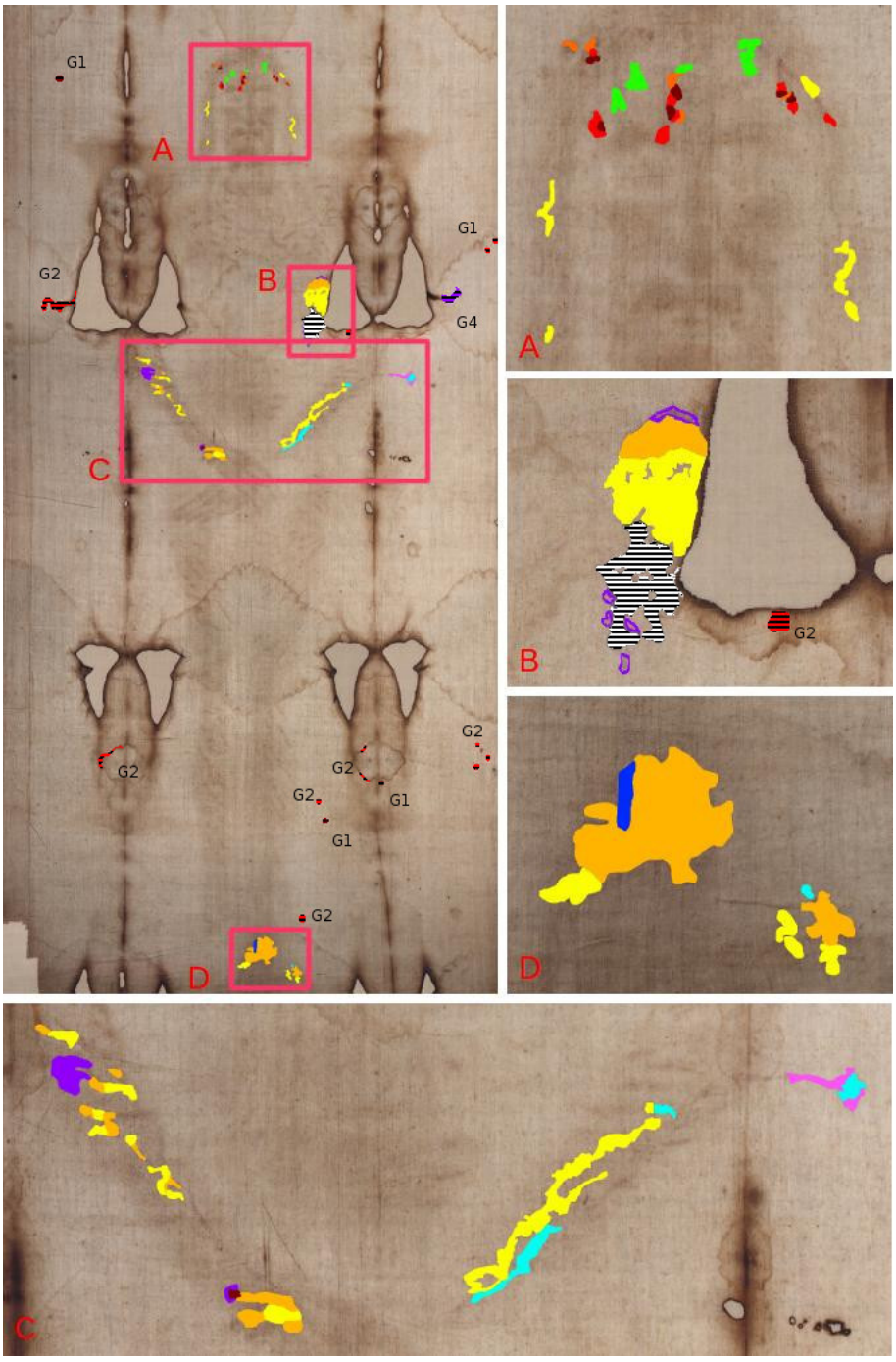

Figure 3. Compatibility areas for the frontal image in reference to Figure 5.

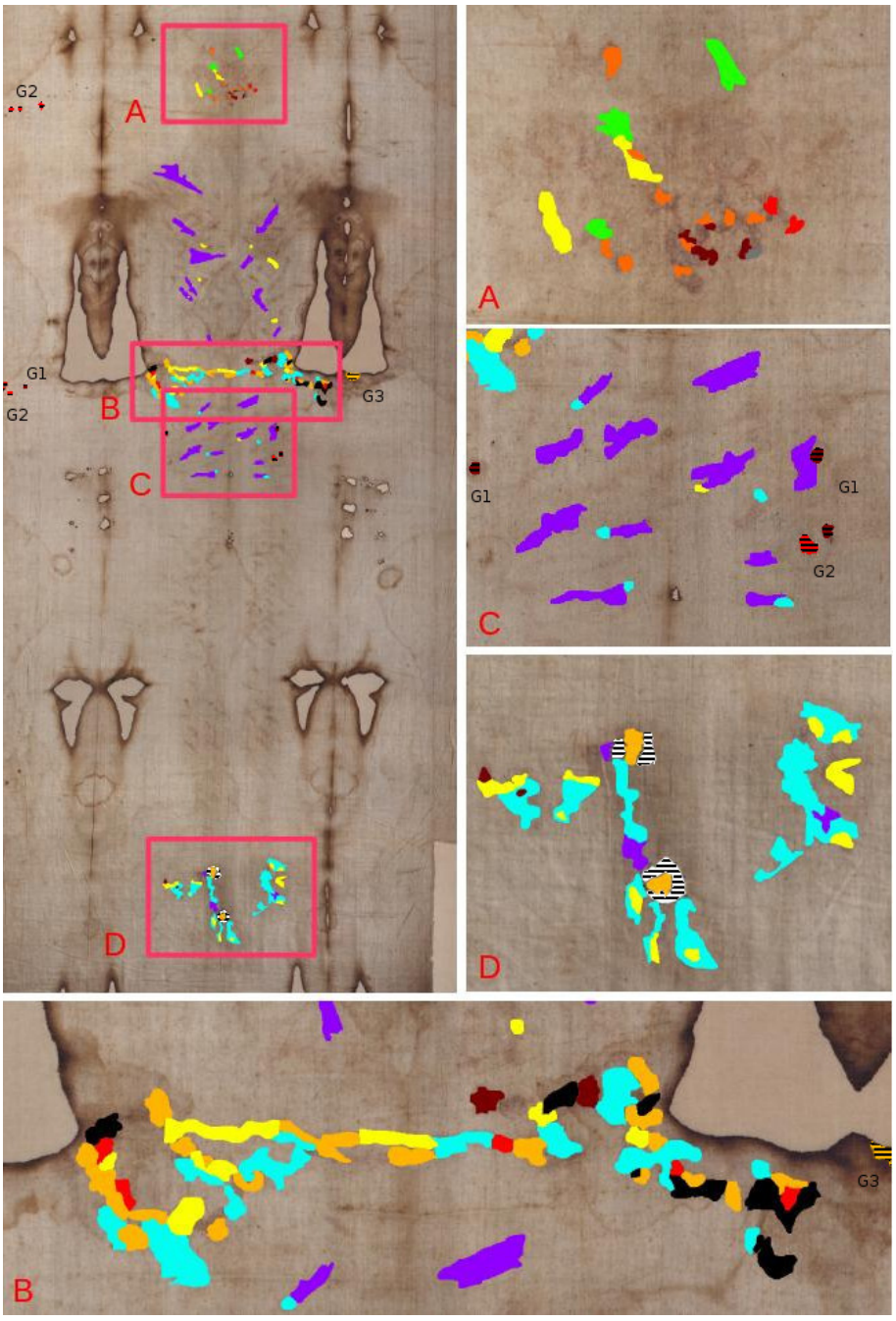

Figure 4. Compatibility areas for the dorsal image in reference to Figure 5.

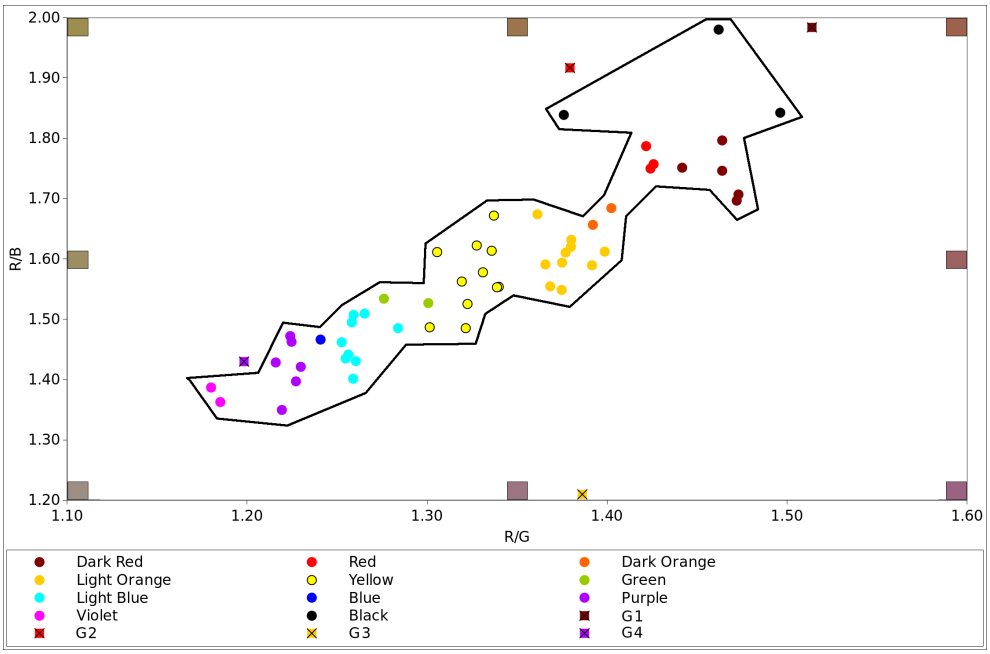

Figure 5. Numerical ratios of the different compatibility zones of Figures 3 and 4. Eight colored squares are added near the graph edges to allow the comparison with real colors.

Table 1. Reference colors with maximum and minimum ratios.

Color	R/G min	R/G max	R/B min	R/B max
Dark Red	1.44	1.47	1.70	1.80
Red	1.42	1.43	1.75	1.79
Dark Orange	1.39	1.40	1.66	1.68
Light Orange	1.36	1.40	1.55	1.67
Yellow	1.30	1.34	1.49	1.67
Green	1.28	1.30	1.53	1.53
Light Blue	1.25	1.28	1.40	1.51
Blue	1.24	1.24	1.47	1.47
Purple	1.22	1.23	1.35	1.47
Violet	1.18	1.19	1.36	1.39
Black	1.38	1.50	1.84	1.98

The ratios spotted as G1 and G2, respectively R/G 1.51±0.06 - R/B 1.98±0.06 and R/G 1.38±0.02 - R/B 1.92 ± 0.03, are not compatible with the above-mentioned blood ratios since they are too high. The G3 group, whose ratios are R/G 1.39 ± 0.45 - R/B 1.21 ± 0.34, presents instead too low values. Only one ratio, named G4, with ratios (R/G 1.20 ± 0.17 - R/B 1.43 ± 0.27), is included in the range from minimum to maximum values of above-mentioned classes: for these reasons, it could be denoted as a bloodstain.

4 Formation Hypothesis

The different ratios presented the Section 3 were categorized by considering their respective position to produce an hypothesis on the stain formation. Six categories were found and their ratios were shown in Figure 6. An unambiguous attribution for each ratio to a category is not however completely possible. Therefore, a detailed analysis was reported for each group, highlighting common aspects and differences from other stains. Table 2 shows the link between categories and ratios.

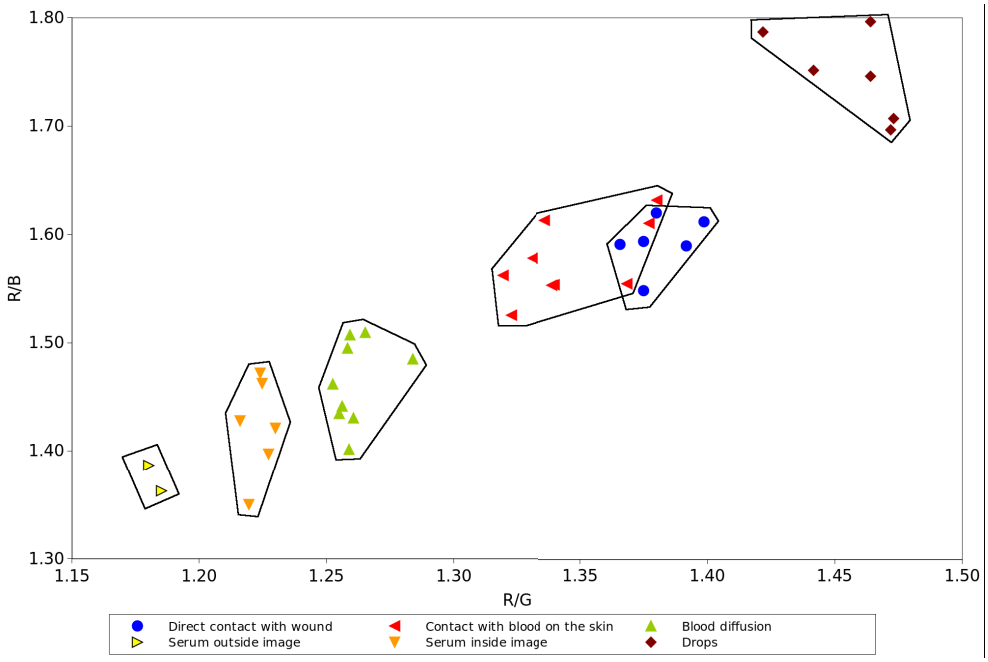

Figure 6. Compatibility zones ratios linked to categories.

Table 2. Association between categories and colors, with reference to maximum and minimum ratio values.

Color	R/G min	R/G max	R/B min	R/B max
Direct contact with wound	1.37	1.40	1.55	1.62
Contact with blood on the skin	1.32	1.38	1.53	1.63
Blood diffusion	1.25	1.28	1.40	1.51
Serum outside image	1.18	1.19	1.36	1.39
Serum inside image	1.22	1.23	1.35	1.47
Drops	1.42	1.47	1.70	1.80

(a) Direct contact with wound

Red ratios are very high; these zones are delimited and localized. Red distribution is, in fact, homogeneous. Considering the particularity of these stains, it is possible to suppose that these zones of the sheet came in direct contact with the wounds of the MS, absorbing relatively large amounts of blood: they were covering the wounds. This hypothesis explains the homogeneity of the color.

(b) Contact with blood on the skin

A separation between lines with a different shade of red can be noticed with a visual analysis. Red ratios are a lower than the previous category ones. These results allow to hypothesize that the blood was still liquid but in lower concentration than (a): the blood does not tend to be uniform, but it generates drops in order to lower its superficial energy, gathering in zones that can hold larger amounts of liquid. These considerations lead to hypothesize that the blood of these zones was originally deposited on the skin of the MS; in a second time it was absorbed by the sheet following a process named ”fibrinolysis” [20].

(c) Blood diffusion

Ratios are lower than in (a) and (b) and this leads to hypothesize that in these zones the sheet did not cover wounds or blood deposits of the skin of the MS: the blood probably migrated by capillarity from zones where blood presence was larger.

(d) Serum

Ratio values in these zones are sensibly lower than in the other categories and similar to background ones. Anyway, because of their location near the previous zones and their shapes, it is possible to suppose that these stains were ”Serum”. Serum has minor viscosity of blood, causing its major diffusion in the flax sheet. Its slight red coloring induces to assume a scarce presence of hemoglobin. Ratio values are similar, but two main groups of serum can be highlighted, linked to their position on the surface of the sheet:

- Serum inside image: higher ratios;
- Serum outside image: lower ratios.

Different ratio values can be explained by the theory of the body image formation based on corona discharge [21]: energy from the inside of the body altered the blood composition of the nearer stains inside the image.

(e) Drops

Typical ratios of these category are the highest of the whole sheet. Interested zones are very localized and their shapes induce to assume that their formation was linked to blood gathering caused by geometrical or physical factors: the blood can’t slide in any directions and it stopped in a zone, forming a ”sac” of coagulated blood, very dark.

5 Conclusions

This work presents the results of a chromatic analysis performed on the stains of the Shroud of Turin from a high definition photograph taken in 2002 by G. Durante. The analysis is followed by hypothesis on their formation based on their position and their chromatic values.

The analysis through chromatic ratios revealed to be effective, providing a chromatic map highlighting analogies and differences among the different stains in the cloth. The ratios allowed to define the boundaries to identify the blood presence. Compatibility tables were compiled to provide comparison values which can be suitable for the etiology study.

Considering the previous results, hypotheses about stain formation were drawn. Six categories were found, which were created by considering decreasing values of ratios linked to an increasing distance from the blood source.

Acknowledgment

The authors would like to thank Prof. Giulio Fanti, University of Padua, for suggesting the original research idea, the precious help and support during the work, the provided material and the review of the paper.

Nomenclature

i_q [−]	standard deviation of the ratio
i_{xi} [−]	standard deviation of the average chromatic value
K [−]	standard deviation extension factor
q [−]	chromatic ratio
q_{RG} [−]	Red/Green (R/G) ratio
q_{RB} [−]	Red/Blue (R/B) ratio
x_i [−]	average chromatic ratio
Θ_i [−]	sensibility rate

References

[1] P. E. Damon, D. J. Donahue, B. H. Gore, A. L. Hatheway, A. J. Timothy Jull, T. W. Linick, P. J. Sercel, L. J. Toolin, C. B. Ramsey, E. T. Hall, R. E. M. Hedges, R. Housley, I. A. Law, C. Perry, G. Bonani, S. E. Trumbore, W. Woelfli, J. C. Ambers, S. G. E. Bowman, M. N. Leese, M. S. Tite, "Radiocarbon dating of the Shroud of Turin", Nature, 337(6208), 611-615 (1989).

[2] G. Fanti, P. Baraldi, , R. Basso, A. Tinti, "Non-destructive dating of ancient flax textiles by means of vibrational spectroscopy", Vibrational Spectroscopy, Volume 67, pp. 61-70 (2013).

[3] G. Fanti, P. Malfi, "Multi-parametric micro-mechanical dating of single fibers coming from ancient flax textiles", Textile Research Journal (2013), SAGE Pub., Volume 84 Issue 7 May 2013.

[4] G. Fanti, P. Malfi, "A New Cyclic-Loads Machine For The Measurement Of Micro-Mechanical Properties Of Single Flax Fibers Coming From The Turin Shroud", AIMETA Congress, Turin, Italy (2013) http://shroudofturin.files.wordpress.com/2013/09/aimeta-fanti.pdf

[5] G. Fanti, "Hypotheses regarding the formation of the body image on the Turin Shroud. A critical compendium", J. of Imaging Sci. Technol., Vol. 55, No.6, p. 060507 (2011).

[6] G. Fanti, "Can Corona Discharge explain the body image formation of the Turin Shroud?", J. of Imaging Science and Technology, Vol. 54, No. 2, pp. 020508-1/10 (2010).

[7] Fanti, R. Maggiolo, "The double superficiality of the frontal image of the Turin Shroud", J. of Optics A: Pure and Applied Optics, volume 6, issue 6, 2004, pp. 491- 503.

[8] G. Fanti, R. Basso, G. Bianchini, "Turin Shroud: Compatibility Between a Digitized Body Image and a Computerized Anthropomorphous Manikin", J. of Imaging Sci. Technol., 54 No.5, p. 050503-1/8, (2010).

[9] M. Bevilacqua, G. Fanti, M. D'Arienzo, A. Porzionato, V. Macchi, R. De Caro, "How was the Turin Shroud Man crucified?", Injury Vol. 45 Supp. 6 pp. S142-S148 (2014), http://dx.doi.org/10.1016/j.injury.2014.10.039 (accessed August 2015).

[10] G. Fanti, P. Malfi, "The Shroud of Turin – First century After Christ!", Pan Stanford Publishing Pte. Ltd., Singapore, 2015.

[11] Faccini B., Carreira E., Fanti G., De Palacios J., Villalain J., "The Death Of The Shroud Man: An Improved Review", Proc. Int. Conf.: The Shroud Of Turin: Perspectives on A Multifaceted Enigma, Ohio USA (2008), Libreria Progetto, Padova, Italy (2009), www.ohioshroudconference.com/papers/p07.pdf

[12] F. T. Zugibe, "The Crucifixion of Jesus: A Forensic Inquiry", 1st ed.; M. Evans and Company: New York (2005).

[13] McCrone, Walter C. Judgement Day for the Turin Shroud", pp. 5-12, Chicago: Microscope Publications, (1996).

[14] A. D. Adler, "Updating recent studies on the Shroud of Turin", American Chemical Society, Symposium Series No. 625, Archaeological Chemistry 625, 223-228, (1996).

[15] P. Baima Bollone, M. Jorio, A. Lucia Massaro, "La dimostrazione della presenza di tracce di sangue umano sulla Sindone", Sindon 30, 5 (1981).

[16] E.J. Jumper, Adler A.D., Jackson J.P., Pellicori S.F., Heller J.H., Druzik J.R., "A comprehensive examination of the various stains and images on the Shroud of Turin", Archaeological Chemistry III, ACS Advances in Chemistry n° 205, J.B. Lambert, Editor, Chapter 22, American Chemical Society, Washington D.C., 1984, pp. 447-476.

[17] http://www.gimp.org/, accessed on January 1st, 2008.

[18] Evaluation of measurement data – Guide to the expression of uncertainty in measurement JCGM 100:2008.

[19] G. Bedon, M. Linguanotto, L. Simonato, F. Zara, "Study of the bloodstains in the Shroud of Turin. International Congress", Int. Conf. The Shroud Of Turin: Perspectives on A Multifaceted Enigma, Ohio State University, (2008), Libreria Progetto, Padova, Italy (2009). https://sites.google.com/site/bloodstainsstudies/

[20] C. Brillante, "La fibrinolisi nella genesi delle impronte sindoniche", "La Sindone, Scienza e Fede", Atti del II Convegno Nazionale di Sindonologia, Bologna 27-29 Novembre 1981, CLUEB, Bologna 1983, pp. 239-241.

[21] G. Fanti, F. Lattarulo, and O. Scheuermann. "Body image formation hypotheses based on corona discharge." Third Dallas International Conference on the Shroud of Turin: Dallas, Texas. 2005. www.ohioshroudconference.com/papers/p15.pdf